Research Article

Mineralogical composition and C/N contents in soil and water among betel vineyards of coastal Odisha, India

Biswajit Patra[1,2] · Ruchita Pal[3] · R. Paulraj[2] · Surya Narayan Pradhan[1] · Ramovatar Meena[2]

© Springer Nature Switzerland AG 2020

Abstract

The *Piper betle* L. leaves and their significance were described in various ayurvedic studies of India and China for its diverse use in cultural practices and treatment of various health disorders. The leaves of *P. betle* were used as post-meal mouth freshener in India for centuries. However, it offers economic benefits to farmers of Coastal India at large. Betel leaves cultivated agricultural soils play a significant role for their mineralogical composition. So, this present study aimed to find out the soil physicochemical characteristics and C/N contents of Betel vineyards of coastal Odisha. The soil and water samples were collected from local varieties of *P. betle* L. cultivated vineyards of Balasore, Ganjam, and Puri districts of Odisha and investigated their mineralogical composition. The soil mineralogy plays crucial role to understand the soil–plant relations. Coastal soil samples also contain the most prized mineral aggregations from economical perspectives. The mineralogical composition involves chemical composition, essential elemental composition, and surface morphology. The mineralogical and elemental composition of soil samples were carried out by using various techniques like Fourier transform infrared spectroscopy, X-ray diffraction (XRD) and energy-dispersive X-ray fluorescence, scanning electron microscopy attached with energy-dispersive X-ray system. CHNS analyzer for quantification of hydrogen, nitrogen, carbon, and sulfur content. H_2O_2 (30%)-treated soil is employed to eliminate the organic carbon from mass soil samples. The scanning electron microscopy analysis revealed the presence of heterogeneity shape and size of surface soils of both treated and untreated soils. For estimation of total organic carbon (TOC), inorganic carbon, total nitrogen, and total carbon, water samples were analyzed through TOC analyzer. Percentage variation arises in GAN and PUR sites soil due to more assumption of organic matter from clay soils in comparison with sandy soils of BAL. The spectra of FTIR point out Kaolinite and Quartz as the key components and others are minor components. The common minerals like quartz, hematite, kaolinite, montmorillonite, calcite, organic matter and illite in diverse compositions are recognized. Further, the presence of these above minerals was confirmed by the XRD analysis. Morphological analysis of kaolinite indicated euhedral, hexagonal, and pseudo-hexagonal-shaped plates. The mineralogical data revealed the relative abundance of phosphorus and nitrogen was less in all soils. Depletion of P and N may be resulted due to introduction of fresh plowed soil from grazed pastoral land. The present research uncovers that soils requires adequate input of additional compost, manures, and fertilizers for maximal vegetative growth and economic yield as well. As *P. betle* species is very precious medicinal plant, and this research suggested not to use contaminated water for betel cultivation. Our results also helpful for the improvement in soil management in the vineyards to determining the mineral nutrients that affect plant growth and development.

Keywords Mineral composition · Soil chemistry · Betel vineyards · Soil morphology

---

✉ Ramovatar Meena, rammeenarv@gmail.com; Surya Narayan Pradhan, likesnp@gmail.com | [1]School of Life Sciences, Sambalpur University, Jyoti Vihar, Odisha 768019, India. [2]School of Environmental Science, Jawaharlal Nehru University, New Delhi 110067, India. [3]Advanced Instrumentation Research Facilities, Jawaharlal Nehru University, New Delhi 110067, India.

1 Introduction

Soil profile variation among intra and inter-regional agroecosystem provides information not only about characteristics and individuality perspective but also frequent anthropogenic interferences. Coastal soil is the most significant and formed due to natural weathering. Pedogenesis is an ever-evolving process [1, 2]. Soil has complex buffering capacity which is advantageous to sustenance of human and other living fauna and flora [3]. Increased utilization of pesticides in small scale agricultural field can threat to ecosystem [4]. The typical weather and other edaphic factors also influence the distribution of coastal soil. So understanding the procedure of soil concoction response is basic for regulating agro biological system from territorial to worldwide scale [5–7]. The evaluation of soil forms can be gauged by the breakdown of physically happening minerals, stones, animal matter and growth of plants. Likewise, it also incorporates the recognition of particles from engineered composts to various forms of phosphate, nitrate and sulfate as ecological antiques [8]. Soil profile is modulated by countless dead and decaying materials of plants and animals and anthropogenic origin [9, 10]. Standardization of soil appraisals is troublesome as a result of assorted variety and un-homogeneity of soil tests [11].The mineral investigation gives prompt territory of research. The most significant ramifications of soil contaminants are pesticides, hydrocarbons, herbicides, and chlorinated hydrocarbons [10]. Soil characteristics have the most significant biological excellence than air and water [12]. Interestingly, soil quality was not restricted to the level of soil contamination. Soils regularly respond to altered land utilization [13–16]. In this manner, a significant constituent of soil reflects the soil superiority. Sandy soils were utilized in agrofarms in numerous geographical areas of the globe [17, 18]. Moreover, soils show more porousness and less water absorbance tendency [19–21]. Sandy loam soils differ in their synthetic and morphological factors to a large extent [18, 22]. The principal sources of soil varieties were due to topography and edaphic factors [2, 18, 23–25]. Understanding the physicochemical properties of soil helps to opt the best soil for crop improvement [26–28]. The soil's capacity to provide water for plant life is an element of the water maintenance, whose consequences from the association between mineralogy, surface, cropping systems, organic fractions, and the administration rehearses [29]. Soil organic Carbon stockpiling was affected by the integrity between carbon contribution, from plant deposits or animal excreta. Changes in soil dampness, nitrogen substance (N), and temperature can prompt significant alteration in soil breath and total carbon [30]. Soils accumulate according to environment and measures of carbon content (C) as natural issue. Moreover, postponed advancement revives the disintegration of soil regular issue and the effect the damage of 20% to 67% of the soil carbon in an agrarian plot [27, 31]. However, rebuilding of high plant assorted variety may enormously expand carbon catch and capacity rates on corrupted and deserted cultivating lands [32, 33]. Nitrogen contribution to agricultural field, atmospheric nitrogen deposition affects the net CO_2–N_2O contribution impacting nitrogen advancement [10]. Its deposition rates are increasing worldwide due to fossil fuel and compost use [34]. It also expected to invigorate soil N_2O discharge [35]. Phosphorus (P) is a key component for the most part constraining essential creation and yield of harvest plants, which has prompted enormous measures of phosphate manure in agri-business at worldwide scale [36]. Mineralization is a physiological progression, which comprises the mineral deposition in a natural setup. Minerals are composed of generally calcium. Mineralization is a complex and multi-staged procedure requiring associations of numerous physicoedaphic factors.

Water is the most significant regular assets on the earth. As a result of its multifarious use, water is indispensible for existence of human society and nature and there are expanding clashes between limiting human water deficiencies and sustaining healthy ecosystem [37]. This is quite obvious that whole plant water use and productivity viably depicts the connection among carbon and water trade at a significant level that was pertinent to all the improved plant rivalry and biological systems responses to water deficiencies [38]. Various methodologies have been created to survey the water quality. These strategies incorporate the examination of various parameters like pH, conductivity, total organic carbon (TOC), turbidity, and total dissolved solids (TDS). TOC is the sum of carbon originating from natural chemical composite and utilized as inexplicit marker of water quality [37]. The biochemical oxygen demand test has conventionally been utilized in water analysis because of issues of repeatability and restraint by regularly occurring water ions and compounds, is as often as possible supplanted by the chemical oxygen demand test for water monitoring, modeling, design and plant operational investigation [10]. The BOD test is a five day experiment whereas COD outcomes finished around that day. Likewise, COD experiment is unchanged by the nearness of poisonous substances accomplishing good accuracy and consistency, in spite of fact that chloride (Cl^-) can hamper the test at higher density [39]. However, conventional methods have various disadvantages. So, analysis of total organic carbon with modern instruments has essential [34]. TOC is the possible option to both BOD

and COD experiments and conceivably extra demand than COD experiment [18, 40]. Recently TOC is considered as a potential substitution of COD and BOD analysis [41]. Additionally, TOC has significant role to monitor overall levels of organic compounds present in water, and it has also utilized as potent indicator of qualitative water assessment [42].

1.1 Study area

The coastal villages of different districts (Balasore, Puri,and Ganjam) were selected for the study. Soil and water samples were collected from *Piper betle* cultivated vineyards of Bahalia revenue area of Bhogarai block of Balasore (21°39'0.09"N87°27'0.6"E), Torihan Bondha of Nimapada block of Puri (20.06°N85.93°E) and Randha of Panchama block of Ganjam (19.23°N 84.76°E) district (Fig. 1). Common varieties of betel leaves, i.e., *Piper betle* var. Bali, *Piper betle* var. Chandrakana, *Piper betle* var. Kala Bangla and *Piper betle* var. Jhanji were found in soils of Balasore, Puri and Ganjam districts respectively (Fig. 1c). The climates of these districts are observed as summer season, dry winter season, high humidity rainy season and average temperature throughout year. Cyclones are frequent in these districts because of the close proximity to the Bay of Bengal.

2 Materials and methods

2.1 Soil sampling and analysis

Soil sampling was done in the year 2017–2018. Top surface soil (upper) and 30 cm depth soil (lower) were collected inside the Betel vineyards (*Boraj*) of study sites. Soil profile characterized by their constituent particles size, morphology and color [43, 44]. Soil organic carbon distribution within soil profile has extremely influenced by diverse natural and anthropogenic practices. The alterations in soil profile by any means will affect soil carbon accumulation in subsequent layers of soil profile. Soil texture analysis can be studied through soil profiling of top 30 cm soil of respective vine yards. Water holding capacity of soil of coastal India is adequate for optimal vegetation of betel vines. Excavation and analysis of top 30 cm soil holds fundamental clue to the nutrient analysis [45, 46]. The sampling process followed by taking out plant material and leaves from the spot before collecting soil samples. The soils gathered by 7 cm diameter of T-shaped iron twist drill up to deepness of 30 cm. A stainless steel flat spatula was utilized for taking soil. Five samples (four different corners and one from center) were utilized to make mixtures, for the selection of better set. These procedures were used for both surface (upper) and 30 cm depth (lower) soil. The soil samples were sieved (< 0.2 mm) and air dried and stored in sterile closed glass bottles for further investigation [11, 47]. Samples were numbered serially and symbolically from 1 to 6 for untreated soils (sample 1 is lower soil of Balasore,
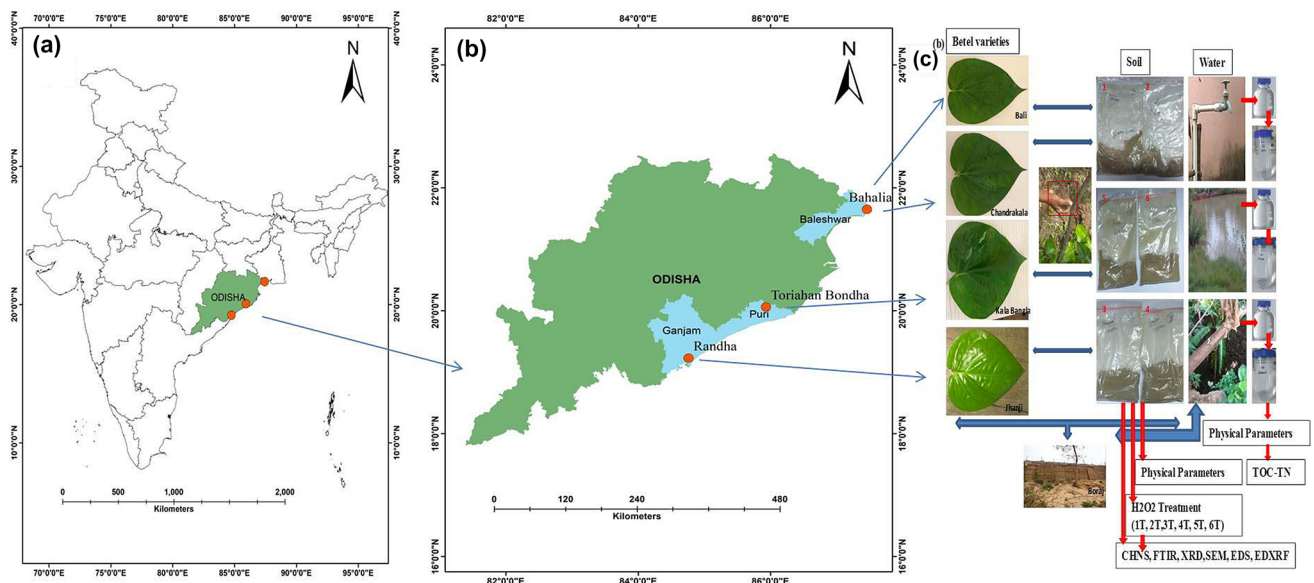

Fig. 1 a, **b** Map of India and Odisha showing the study sites. **c** Graphical representation of characterization of soil and water with specific common betel varieties

2 is surface soil of Balasore, 3 denoted as lower soil of Ganjam, followed by upper soil sample 4, 5 represented as 30 cm depth soil of Puri followed by surface soil sample 6) and 1T to 6T for treated soils (1T and 2T are depth and surface soils of Balasore, 3T and 4T are depth and surface soils of Ganjam and lower and upper soils of Puri are 5T and 6T. pH, electrical conductivity and temperature of soil samples were analyzed by taking direct reading of potable LCD digital pH, temperature, and EC meter. Texture was determined by Bouyouco's method [48, 49]. For estimation of hydrogen, carbon, nitrogen and sulfur percentages, fine homogenized powdered soils were dictated by CHNS analyzer (Model: EuroVector EA 3000 elemental analyzer). H_2O_2 (30%) treated soils were directed to eradicate the natural organic carbon (OC) from mass soil samples. The powdered fine samples (soil) are densely treated with potassium bromide (KBr) pellets (small sphere) and analyzed by FTIR Benchtop system, The Agilent Cary 670 spectrometer. For Fourier transform infrared (FTIR) analysis, spectral scanning obtained at 4000–500 cm^{-1} wave number to evaluate mass soils and H_2O_2 (30%) treatment soil [50–52]. The FTIR peaks were analyzed by Essential FTIR v3.50.185 from Operant LLC, Searchlt-KnowltAll®information system, ID expert from BioRad laboratories, Inc. and IRPal 2.0 table-driven infrared application programming. For SEM–EDS, Soils were set up by scattering dry powder on both sided conductive sticky tape. Tests were covered with carbon by curve release technique for SEM–EDS and the dried soils were gold-coated utilizing gold electroplating machine (Cressington 108, 19-010100) for 120 s. The gold-coated soil samples were viewed in Scanning Electron Microscope (SEM)-Zeiss EVO40. The SEM pictures were examined using the programing Image J. The surfaces of the particles were scanned and the elemental composition with arrangement was determined by energy-dispersive X-ray spectrometry (EDS) attached to SEM. The outcomes were detected and recorded with the Genesis 60E programming [6]. The mineralogical identification of soil samples were further analyzed by X-ray diffractometer (XRD powder) adopting Panalytical X'Pert PRO MPD (PW3040/60) diffractometer with a X' celerator detector having CuKα radiation and a X-ray ceramic tube. The scanning range was 5° to 90° 2θ, 30 mA and 40 kV, 60 s time/step and 0.02° advanced step size, anti-scattering of 1/4° and divergent slit of 1/8°. The experimental spectral patterns were matched with patterns received from the International Centre for Diffraction Data (ICDD) or Joint Committee on Powder Diffraction Standard (JCPDS) data base [53] and Match! Phase identification from powder diffraction 3.8.0.137, crystal Impact, Bonn, Germany programming and High score Plus from Panalytical software also used for investigation. For EDXRF analysis, the samples stored in oven for a day at room temperature and make it into fine powder. Crush 2 g of soil sample in mortar and pestle with 0. 2 g of boric acid. Then homogeneous powders were made into hydraulically pressed pellets using 20 tons pressure for 15 s. Then put the sample in Epsilon 5-PANalytical EDXRF spectroscopy.

2.2 Water sampling and analysis

Water samples were taken from deep bore wells (Balasore), pond (Puri), and well (Ganjam). The samples were numbered with numerical as well as symbol (BAL, PUR, GAN). The samples complying the standard methods of American Public Health Organization (APHA) and American Society for Testing and Materials (ASTM) were analyzed using various calibrated and standard instruments. The pH was measured by using a pocket pH meter (HI98107, HANNA instruments). The pH meter was calibrated and adjusted by pH 4.0, 7.0 and 10.0 standard solutions before initial recording. After each measurement, the probe was washed with deionized water to debar contaminants in the sample. The electrical conductivity and total dissolved solid of the samples was analyzed by utilizing a TDS and EC meter (Model CD-610, HANNA instruments). The turbidity was analyzed by turbidity meter (Model no. 2100P Turbidimeter HACH, Colombia, USA, Arachem (M) Sdn. Bhd.). Temperature is measured by using electronic digital thermometer (Model No. HI98501, Checktemp® CL Celsius) (Table 8). For estimation of total organic carbon (TOC), inorganic carbon (IC), total nitrogen (TN), and total carbon (TC), water samples were analyzed through TOC analyzer (Model: TOC-L/SHIMADZU-01517/Serial No-H544354). TOC concentration is calculated by substracting IC from TC. Potassium hydrogen phthalate of 99.95% analytical grade was used to make a standard TOC curve for calibration [16, 19, 39, 54].

3 Results

3.1 Soil sampling and analysis

The physiochemical parameters of experimental soils were assessed by standard errors of mean and average. The results of soil profile shows that upper and 30 cm depth soils of Balasore study site (BAL) are more acidic than Ganjam study site (GAN) and Puri study site (PUR). However, lower soils are more acidic than upper soil because of heavy rain fail, manure and commercial fertilizers [55]. The varying soil EC is due to the abundance of moisture held by the soil particles [49, 56, 57]. Soil particle size and texture strongly influence EC. Sandy loam soils of BAL shows low conductivity in upper soil, medium conductivity in clay loam soils of PUR and high conductivity in soils of GAN. Top soils give high conductivity in contrast with

Table 1 The percentage of organic carbon and carbon nitrogen ratio of all study sites

Site	OC (%)		C/N ratio (%)	
	Lower	Upper	Lower	Upper
BAL	0.04 ± 0.02	0.05 ± 0.01	2.22 ± 0.02	2.46 ± 0.13
GAN	0.52 ± 0.02	0.44 ± 0.01	3.05 ± 0.23	4.87 ± 0.06
PUR	0.62 ± 0.00	0.60 ± 0.02	6.54 ± 0.33	5.74 ± 0.23

Mean ± SE

depth soils because of moisture content available in protected cultivated vineyards. EC of top soil of GAN range from 0.5 to 0.6 mS cm^{-1} while EC of 30 cm depth GAN soil varied from 0.4 to 0.5 mS cm^{-1}. EC of top soil of BAL varies from 0.3 to 0.4 mS cm^{-1} followed by lower soil 0.2 to 0.3 mS cm^{-1}. Temperature of GAN top soils are higher and varies from 22 to 23 °C while lower soil varies from 19 to 21 °C, followed by BAL top soil 18 to 22 °C and lower soil 15 to 19 °C. Upper soil and lower soils of PUR shows average temperature. Temperatures of upper soils are maximum due to typical variation of soil, cultivation methods and external environmental condition.

3.1.1 CHNS analysis

Carbon, hydrogen, nitrogen, and sulfur (CHNS) are fundamental and essential components of soil. Understanding the strength of the soil in which crops grown is essential for profitable yields. Carbon is significant for energy content while nitrogen is essential for growth [59]. Fertilizers are added to the soils for controlling the carbon/nitrogen (C/N) proportion. Routine assessment of elemental structure of a complex is represented as a weight percentage of each component present in

the compound [25]. TC percentage of PUR soils are maximum (1.0 ± 0.0, and 1.0 ± 0.0) followed by GAN and BAL (Table 2), whereas following H_2O_2 treatment the Mean ± SD percentage of carbon of PUR soils shows 0.4 ± 0.0 (upper), 0.5 ± 0.0 (lower) as compared to GAN 0.2 ± 0.0, 0.2 ± 0.0 and BAL 0.2 ± 0.0, 0.2 ± 0.0, respectively. The organic carbon percentage and carbon nitrogen ratios are depicted in Table 1. In 30 cm depth soil, OC percentage of PUR ranged from 0.6 to 0.7%. Minimum OC percentage 0.04% was recorded from BAL site followed by GAN site. In surface soil, lowest OC percentage was found in BAL site, while the highest OC was found in PUR site. Carbon nitrogen ratio of surface soil of PUR ranged from 5.4 to 6.1%, GAN from 4.7 to 4.9% and BAL 2.2 to 2.6%. Lower soils of PUR (6.5 ± 0.3) recorded Mean ± SD as maximum followed by GAN (3.0 ± 0.2) and BAL (2.2 ± 0.0). Total nitrogen (TN) percentage of untreated soils of GAN site recorded highest Mean ± SD (0.2 ± 0.0) in lower soil and lowest percentage found in the surface soil of BAL site (0.1 ± 0.0). TN percentage of lower soil of BAL shows 0.1 ± 0.0 followed by PUR site 0.2 ± 0.0 and upper soil of PUR site recorded 0.2 ± 0.0 and GAN site 0.1 ± 0.0. After H_2O_2 treatment, mean ± SD percentage of nitrogen of GAN site decreases (0.1 ± 0.0) and percentage of upper soil of BAL site increases (0.1 ± 0.0). Percentage of TS maximum (4.0 ± 0.0) in upper soils of PUR site followed by lower soil (3.3 ± 0.3) and minimum percentage (0.1 ± 0.0) recorded in BAL site surface soil followed by depth soil (0.1 ± 0.0). After H_2O_2 treatment, Mean ± SE percentage of sulfur decreases in GAN and PUR site soils while a little change in BAL soil (Table 3). Percentage variation arises in GAN and PUR sites soil due to more assumption of organic matter from clay soils in comparison with sandy soils of BAL.

Table 2 The percentage of total carbon, total nitrogen, and total sulfur content of all study sites

Site	TC (%)		TN (%)		TS (%)	
	Lower	Upper	Lower	Upper	Lower	Upper
BAL	0.29 ± 0.01	0.29 ± 0.01	0.13 ± 0.01	0.12 ± 0.01	0.16 ± 0.01	0.14 ± 0.01
GAN	0.76 ± 0.02	0.66 ± 0.01	0.25 ± 0.02	0.14 ± 0.01	0.45 ± 0.01	0.69 ± 0.01
PUR	1.09 ± 0.01	1.07 ± 0.01	0.17 ± 0.01	0.19 ± 0.01	3.30 ± 0.32	4.05 ± 0.01

Mean ± SE

Table 3 The percentage of inorganic carbon, inorganic nitrogen and inorganic sulfur content of all study sites

Site	IC (%)		IN (%)		IS (%)	
	Lower	Upper	Lower	Upper	Lower	Upper
BAL	0.25 ± 0.02	0.23 ± 0.01	0.15 ± 0.01	0.13 ± 0.00	0.16 ± 0.01	0.15 ± 0.01
GAN	0.23 ± 0.01	0.23 ± 0.02	0.09 ± 0.01	0.12 ± 0.02	0.16 ± 0.01	0.25 ± 0.01
PUR	0.46 ± 0.01	0.47 ± 0.02	0.13 ± 0.03	0.14 ± 0.01	0.19 ± 0.00	0.13 ± 0.01

Mean ± SE

Table 4 FTIR spectra of untreated soil with respective minerals of all the study sites

Wave number (cm^{-1})						Tentative assignments	Minerals
1	2	3	4	5	6		
–	–	3694.76	3680.62	3701.83	3694.76	Plane declined vibration of H$_2$O	Kaolinite
3615.43	–	3616.98	3609.91	3624.05	3631.12	Internal hydroxyl group of O–H stretch	Kaolinite
–	–	–	–	3305.86	3305.86	H$_2$O molecules stretching H–O–H	Montmorillonite
1631.45	1637.13	1601.78	1630.06	1630.06	1637.13	H–O–H stretching	Illite
1463.79	–	–	–	–	–	CaCO$_3$ asymmetrical bending vibration	Calcite
1093.54	1071.46	–	–	–	–	Si–O-band	Quartz
1009.71	–	1000.76	1000.76	986.61	993.68	Si–O stretching (clay minerals)	Kaolinite
–	–	901.76	901.76	894.69	915.9	Al$_2$O–H deformation	Kaolinite
786.16	774.488	767.41	760.34	774.48	767.41	Si–O stretching	Quartz
660.41	689.63	682.56	696.7	682.56	682.56	Si–O stretching	Quartz
531.66	532.91	–	–	–	–	Si–O–Al (or) Fe$_2$O$_3$	Hematite

Table 5 FTIR spectra of treated soil with respective minerals of all the study site

Wave number (cm^{-1})						Tentative assignments	Minerals
1T	2T	3T	4T	5T	6T		
–	–	3708.9	–	3694.76	3694.76	Plane declined vibration of H$_2$O	Kaolinite
–	3631.12	3624.05	3622.4	3616.98	3631.12	Internal hydroxyl group of O–H stretch	Kaolinite
–	–	–	–	3334.14	3277.58	H$_2$O molecules stretching H–O–H	Montmorillonite
–	1630.06	1622.99	–	1630.06	1630.06	Stretch H–O–H	Illite
1057.32	1078.54	1007.83	1078.3	979.54	986.61	Stretching Si–O(Clay)	Kaolinite
–	–	894.69	908.69	908.83	894.69	Al$_2$O–H deformation	Kaolinite
767.41	767.41	767.41	767.35	781.55	760.34	Stretching Si–O	Quartz
682.56	689.63	689.63	689.61	682.56	682.56	Stretching Si–O	Quartz

3.1.2 FTIR analysis

Fourier transform infrared (FTIR) absorption spectra of H$_2$O$_2$ treated and untreated soil samples of surface layer and 30 cm depth soils were analyzed in reference to available library files. The observed wave number from all the spectra was given in Tables 4 and 5 with corresponding matching and coordinating mineral names. The common minerals like quartz, hematite, kaolinite, montmorillonite, calcite, organic matter, and illite in diverse compositions are recognized. The spectra of FTIR point out Kaolinite and Quartz as the key components and others are minor components. In Puri site, surface and depth soils recorded a wide retention band at 3305.9 cm^{-1} in the range proposes the chance of water due to association in absorbent. However, the chief component of clay is kaolinite which provide the pointed absorption spectral band and appear in all samples shows the existence of organic materials [11, 58].The strong absorption band was observed because of Si–O stretching of Kaolinite and vibration showed in the quality of Illite [11]. Figure 2 shows the comparative line graph indicates FTIR spectras of treated and untreated

soil samples which justify the variations due to H$_2$O$_2$ treatment. Moreover, FTIR of H$_2$O$_2$ treated soil portrayed variation and nearness of organic compound in inflexible form [52]. In untreated depth soil of Balasore soil the frequency of 1463.79 cm^{-1} was because of (CO$_3$)$^{2-}$ stretching vibration. The mineral composition of silicate is essential concern as a result of their importance. In all study samples, Quartz (SiO$_2$) was present. The strongest structural bond of silicate was Si–O bonds and seen in IR spectra of region 900–1100 cm^{-1} was due to stretching in the 400–800 cm^{-1} intense bands region. The Quartz in the soil was recognized with spectral bands and the IR absorption peaks were reported by several authors [59]. Calcite is the form of CaCO$_3$ (calcium carbonate) in the soil. Crystals of Calcite showed trigonal–rhombohedral, that indicated CaCO$_3$ frequencies correlations correspond to the study of Chester and Elderfield [60]. Kaolinite is electrostatically neutral and has triclinic symmetry. A distinctive kaolinite with an structural configuration of Al$_2$Si$_2$O$_5$ (OH)$_4$ was reported by Li et al. [61]. Hematite is in the form of Iron Oxide (Fe$_2$O$_3$) and it solidifies the rhombohedral framework. It has also similar structure like Corundum and Limonite. The spectra
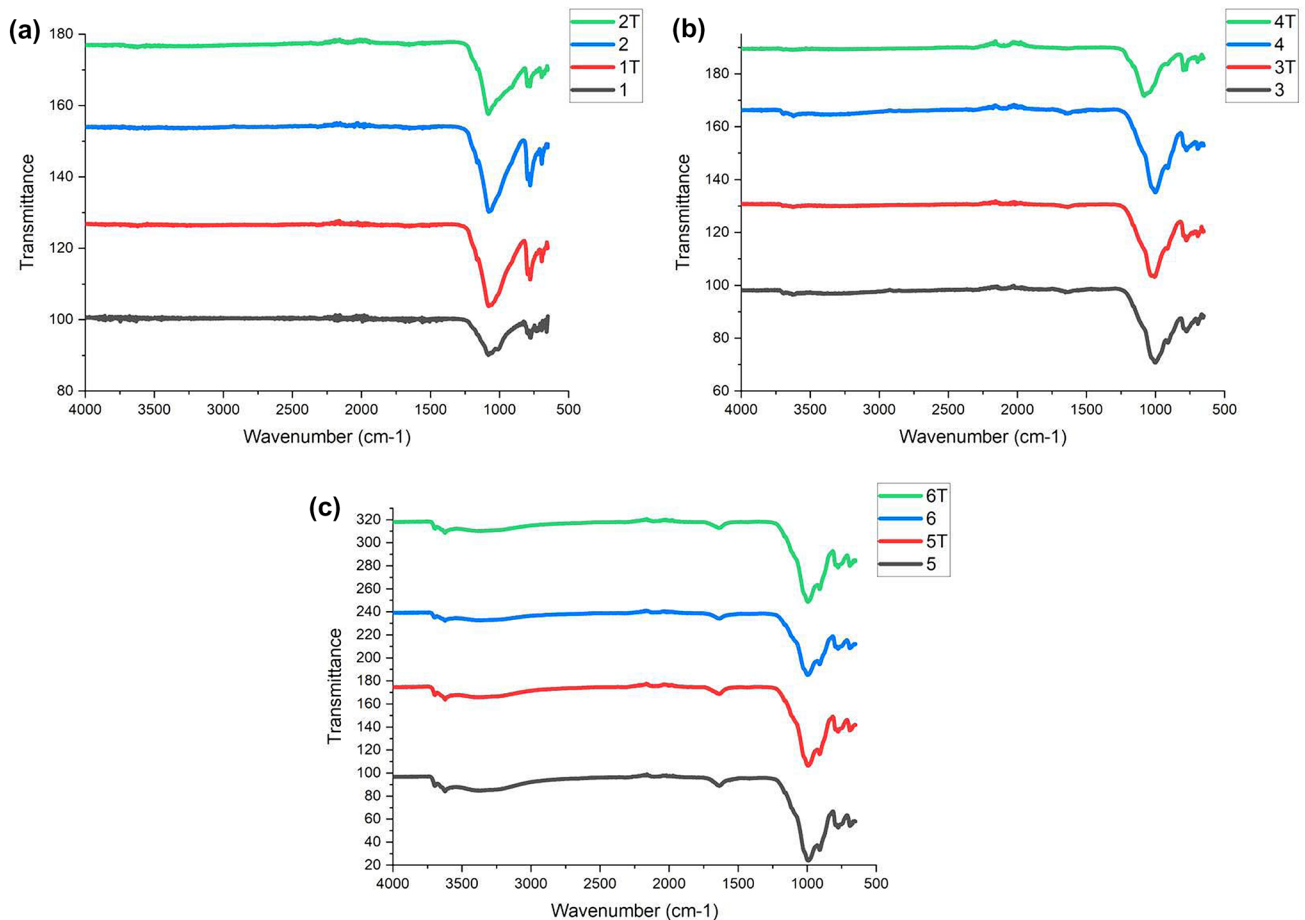
Fig. 2 FTIR spectral comparisons of untreated and treated soils of **a** Balasore, **b** Ganjam and **c** Puri site. (1 and 2—untreated lower and upper soil of Balasore, 1T and 2T—treated lower and upper soil of Balasore; 3 and 4—untreated lower and upper soil of Gan- jam, 3T and 4T—treated lower and upper soil of Ganjam; 5 and 6— untreated lower and upper soil of Puri, 5T and 6T—treated lower and upper soil of Puri)

of Hematite were possible due to Fe–O extended manner of vibration. In these soil samples, the concentrations of Hematite peaks were weak to average. Montmorillonite is an exceptionally delicate phyllosilicate gathering of minerals that regularly structure in tiny crystals. The hypothetical configuration of Montmorillonite is $(OH)_4 \cdot Si_8 \cdot Al_4 \cdot O_{20} \cdot nH_2O$. This is made up of hydrous aluminum silicates as incredibly minute particles. The infrared absorption at 3405 cm^{-1} depicts the existence of Montmorillonite. This may happen because of O–H stretching vibration of H_2O particles [61, 62].

3.1.3 XRD analysis

The X-ray diffraction (powder) is utilized to distinguish the phase identification of crystalline material and give information about mineral composition of soil [63]. In

this technique, some amount of soil samples at all potential directions set in a beam of collimated light emission X-rays of different intensities were checked and recorded consequently to create pattern representing the power of diffracted bar as a function of range 2 Theta (2θ). The presence of minerals in the soil was identified by comparing 2 theta values. The matched standard and overlapped XRD patterns were recorded in Fig. 3 and site wise comparison with untreated and treated soil sample graphs are shown in Fig. 4a–c. From XRD patterns key minerals like kaolinite (K), quartz (Q), hematite (H), illite (I), feldspar (F), calcite (C), and aragonite (A) were identified by comparing with JCPDS data [64]. The observed patterns indicated kaolinite present in the soil as a clay mineral and the nonclay mineral quartz are the major constituents. Further, the presence of these above minerals confirmed the minerals found by the FTIR analysis.
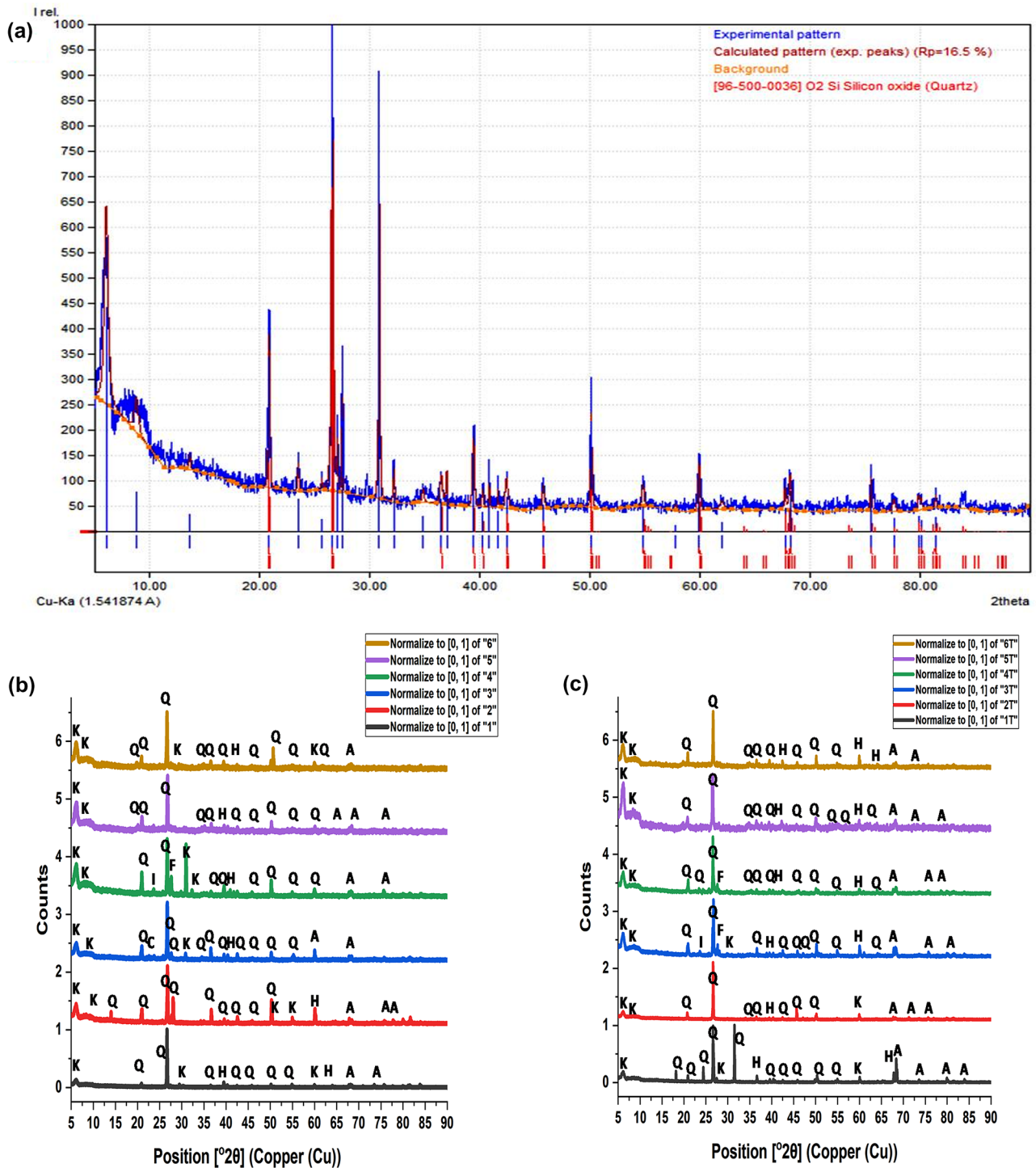
Fig. 3 **a** The experimental and matched patterns of X-ray diffraction spectra of soil sample. X-ray diffraction spectrum depicting mineral patterns of **b** untreated and **c** treated soils. (1 and 2–untreated lower and upper soil of Balasore, 3 and 4-untreated lower and upper soil of Ganjam, 5 and 6-untreated lower and upper soil of Puri; 1T and 2T-treated lower and upper soil of Balasore, 3T and 4T-treated lower and upper soil of Ganjam, 5T and 6T-treated lower and upper soil of Puri)
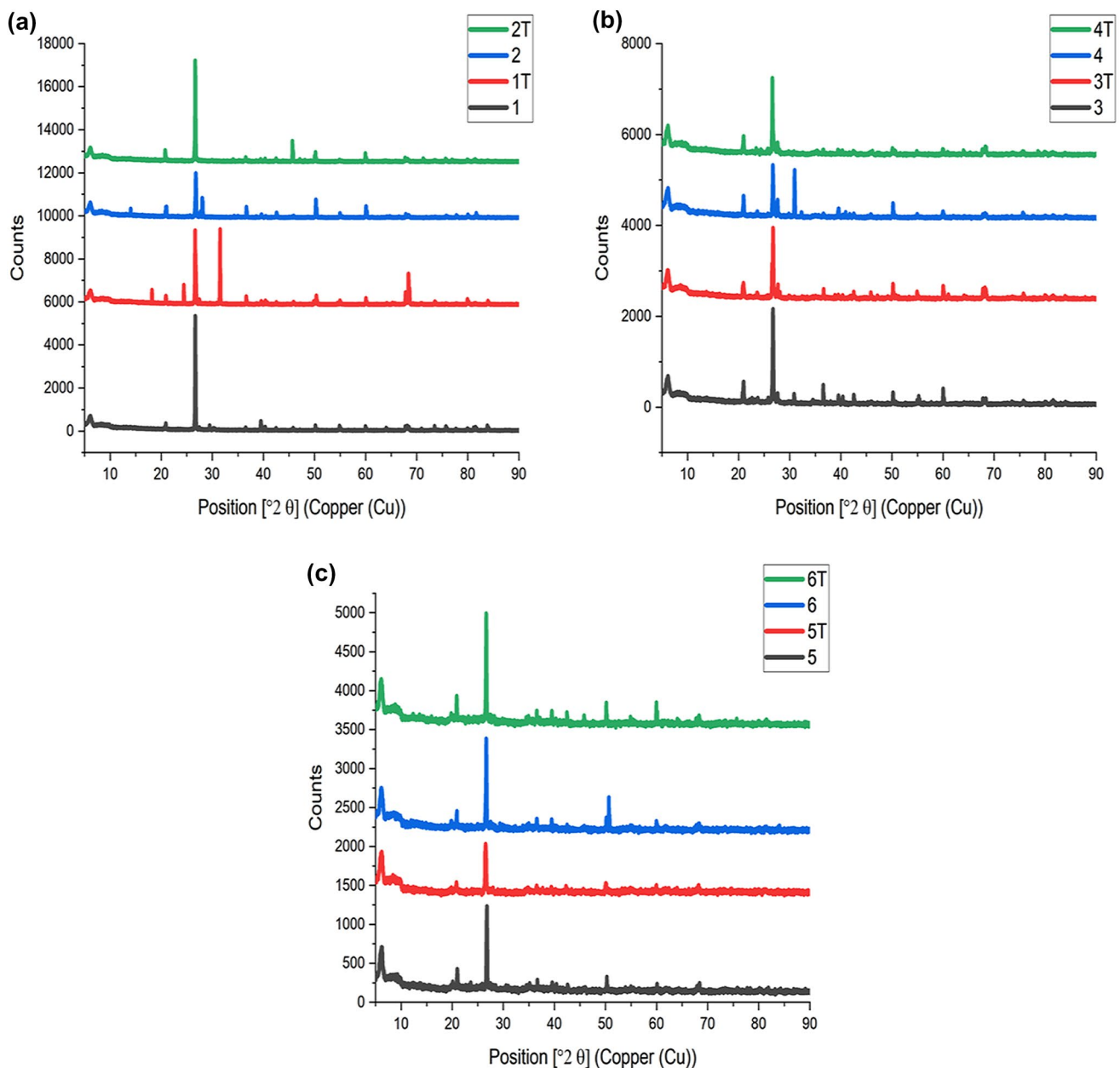
Fig. 4 Compared X-ray diffraction patterns of untreated and treated soils of lower and upper soils of **a** Balasore, **b** Ganjam and **c** Puri. (1 and 2—untreated lower and upper soil of Balasore, 1T and 2T—treated lower and upper soil of Balasore; 3 and 4—untreated lower and upper soil of Ganjam, 3T and 4T—treated lower and upper soil of Ganjam; 5 and 6—untreated lower and upper soil of Puri, 5T, and 6T—treated lower and upper soil of Puri)

3.1.4 SEM analysis

The scanning electron microscopy analysis is a useful technique to portray the soil and rock as thin section analysis has long-established tool for geologist [65, 66]. With SEM, scientist can inspect the bulk mineral composition and potent observation regarding surface [65, 67]. In this investigation, two magnification 100× and 5000× were selected for the soil morphology analysis. Figure 5 showed SEM image of untreated and treated soil sample of Odisha. Sandy loam soil particle of Balasore site lower and upper soils was having well-structured and irregular surface (Fig. 5a) while clay loam soil particle of Ganjam and Puri sites were having compact and smooth surface (Fig. 5b, c) at magnification 100×. Magnification at 5000× shows quartz, kaolinite, calcite, feldspar, and illite in various structure (Fig. 5). It demarcated sporadic, round, triangular and almost triangular for quartz; platy
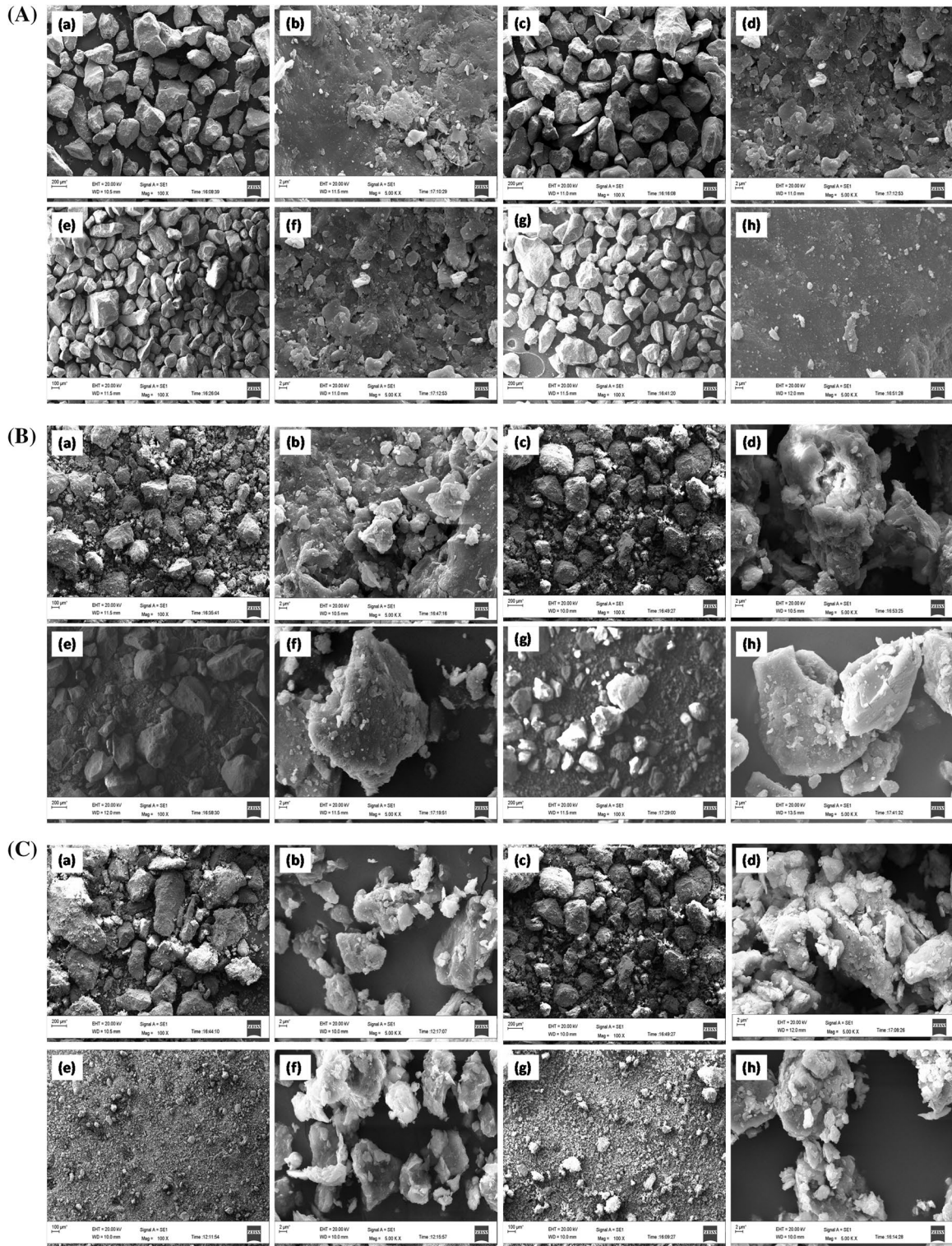
Fig. 5 **a** SEM images of sandy loam soils observed at specific magnification (×100 and ×5000) of Balasore district soil. a and b (1) are lower soil, c, d (2) are upper soil, e, f and g, h (1T and 2T) are respective treated soil. **b** SEM images of clay loam soils observed at specific magnification (×100 and ×5000) of Ganjam district soil. a and b (3) are lower soil, c and d (4) are upper soil, e, f and g, h (3T and 4T) are respective treated soil. **c** SEM images of clay loam soils observed at specific magnification (×100 and ×5000) of Puri district soil. a and b (5) are lower soil, c and d (6) are upper soil, e, f and g, h (5T and 6T) are respective treated soil
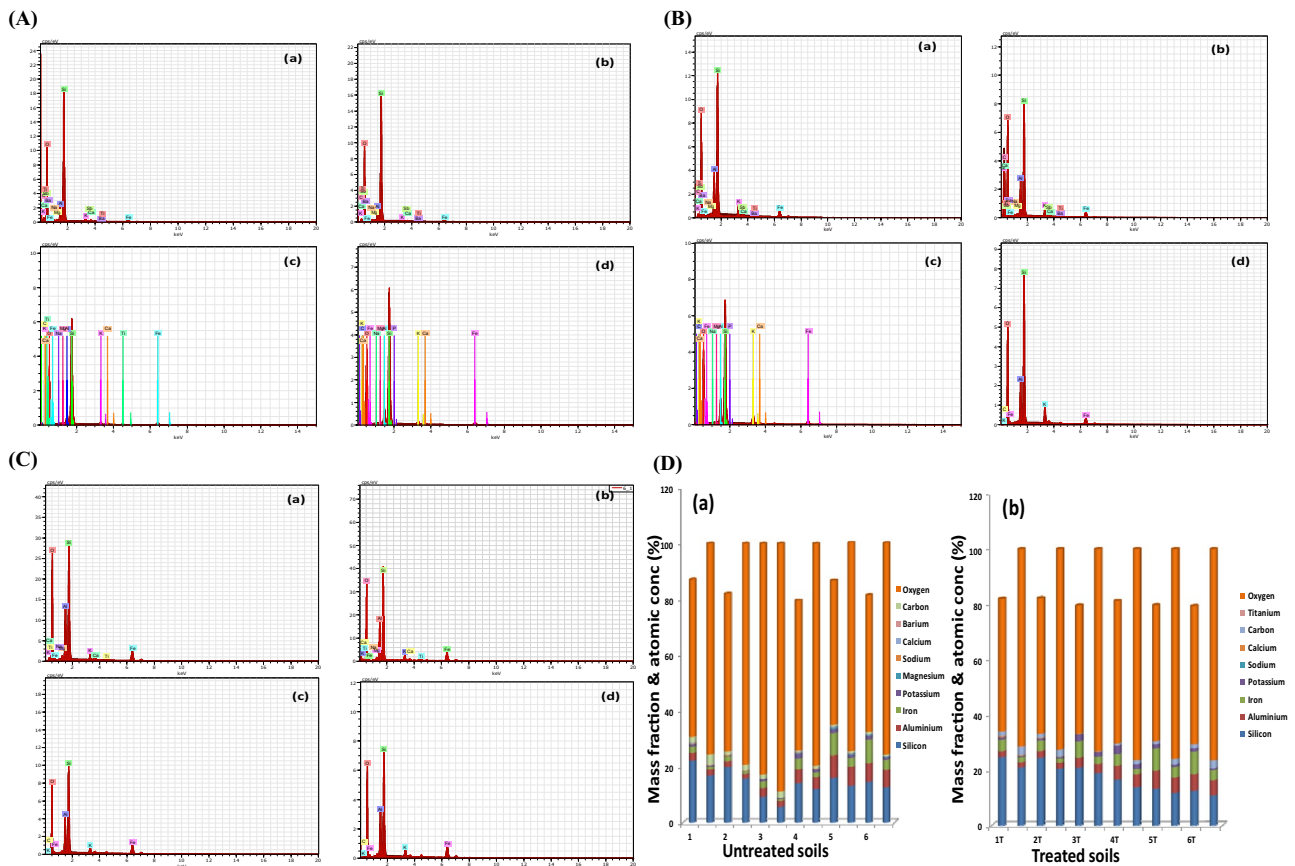
(A)

(B)

(C)

(D)

Fig. 6 **a** SEM–EDS micrographs of soils of Balasore sites. a, b (1, 2) and c, d (1T 2T). **b** SEM–EDS micrographs of soils of Ganjam sites. a, b (3, 4) and c, d (3T, 4T). **c** SEM–EDS micrographs of soils of Puri

sites. a, b (5, 6) and c, d (5T, 6T). **d** Mass fraction and atomic conc. percentage of (a) untreated and (b) treated soils of all study sites

shape for calcite; rectangular, hexagonal, vermiform and flower like appearance for kaolinite in the coastal soil. [17, 69–71]. SEM micrograph of kaolinite indicated euhedral, hexagonal, and pseudo-hexagonal shaped plates [70]. The Quartz full molecules in the SEM image was sporadic form and unpleasant face covered with tiny clay dishes [72]. Euhradral, linear, subhedral curvilinear, and euhedral types Quartz were recognized by study of Stefanie et al. [73]. Scalenohedral and rhombohedral crystal habit of Calcite and prismatic crystal habit of Aragonite twins were distinguished by Gobac et al. [74]. Mineral constituents of untreated and treated soil were further characterized by EDS (Fig. 6).

3.1.5 EDS analysis

Energy-dispersive X-ray spectrometer analysis enables one to identify and confirm the microminerals and inspect the distribution of these minerals within the soils. These individual spectra project additional basic minerals for better comparative scrutiny [17, 65].

However, based on this EDS analysis, the values may be different because of partial-quantitative character of EDS. The information acquired from EDS are not reliable. So, mutually SEM–EDS study gives comprehensive data about the change of surface structure in different soil samples [7, 61, 75]. In our outcomes (Fig. 6), diverse elemental composition in soil, like aluminum (Al), iron (Fe), silicon (Si), potassium (K), sodium (Na), magnesium (Mg), calcium (Ca), barium (Ba), carbon (C), titanium (Ti), and oxygen (O), and their mass fraction and atomic percentage were measured by EDS. Soil samples from different location have different elements, which were analyzed by elemental ratios and types. In all soils the content of Si and O were more because of key elements of Si and SiO_2 (Fig. 5). The contents of aluminum and Sodium were relatively stable in all the sites soil. Mg and Ca content of Ganjam and Puri sites was more as compared to that of BAL sites. But after treatment Mg and Ba are absent in all sites soil samples. The contents of K and Fe in clay loam soil of Puri and Ganjam were maximum than that of sandy soil of Balasore soil.

Table 6 Major and minor element composition of untreated soils of Odisha

Compounds	1	2	3	4	5	6
CO_2	1.24 ± 0.06	7.16 ± 0.08	2.38 ± 0.20	3.16 ± 0.05	5.15 ± 0.45	3.80 ± 0.74
Na_2O	0.00 ± 0.00	0.80 ± 0.05	0.41 ± 0.27	0.66 ± 0.09	0.00 ± 0.00	0.00 ± 0.00
MgO	0.62 ± 0.06	0.56 ± 0.06	0.45 ± 0.05	0.00 ± 0.00	1.48 ± 0.24	1.34 ± 0.20
Al_2O_3	7.16 ± 0.11	6.54 ± 0.61	10.83 ± 0.71	12.45 ± 0.60	15.57 ± 0.39	15.36 ± 0.36
SiO_2	77.92 ± 0.58	72.46 ± 1.48	73.91 ± 1.62	72.31 ± 1.61	64.66 ± 2.10	68.23 ± 0.90
P_2O_5	0.32 ± 0.01	0.23 ± 0.11	1780.37 ± 117.91	0.59 ± 0.47	0.00 ± 0.00	0.0 ± 0.00
S	0.0 ± 0.00	221.82 ± 10.08	242.10 ± 70.73	0.00 ± 0.00	0.0 ± 0.00	0.0 ± 0.00
Cl	0.0 ± 0.00	71.41 ± 17.54	482.66 ± 8.31	375.50 ± 48.25	204.14 ± 16.50	212.31 ± 2.50
K_2O	1.36 ± 0.11	1.96 ± 0.57	3.85 ± 0.12	3.53 ± 0.10	2.34 ± 0.56	2.34 ± 0.56
CaO	1.64 ± 0.01	1.52 ± 0.32	0.87 ± 0.16	0.73 ± 0.02	0.72 ± 0.24	0.69 ± 0.15
TiO_2	4.18 ± 0.16	3.30 ± 0.32	1.48 ± 0.18	1.82 ± 0.08	1.53 ± 0.52	1.14 ± 0.21
MnO	1258.36 ± 457.17	1237.14 ± 136.13	1070.81 ± 15.14	902.13 ± 2.84	0.50 ± 0.43	0.71 ± 0.40
Fe_2O_3	5.16 ± 0.62	2.11 ± 1.41	3.49 ± 0.05	3.77 ± 0.20	8.63 ± 1.10	8.37 ± 1.11
Ni	20.16 ± 0.01	16.71 ± 2.39	15.36 ± 1.57	18.56 ± 0.42	75.89 ± 1.59	65.67 ± 0.91
Cu	26.92 ± 1.55	26.86 ± 2.37	22.36 ± 0.63	23.29 ± 0.59	49.31 ± 1.66	44.19 ± 0.87
ZnO	44.22 ± 1.63	43.38 ± 1.99	54.21 ± 5.83	65.48 ± 0.58	76.40 ± 1.62	68.82 ± 2.02
B	1.60 ± 0.31	1.18 ± 0.06	13.25 ± 0.58	14.44 ± 0.47	20.16 ± 1.81	14.87 ± 2.22
Mo	44.55 ± 0.56	45.53 ± 3.26	25.22 ± 1.27	3.77 ± 0.09	2.86 ± 0.55	1.43 ± 0.18
Se	0.0 ± 0.00	0.0 ± 0.00	226.67 ± 11.23	195.03 ± 1.89	0.00 ± 0.00	0.0 ± 0.00

Mean concentration ± SD

Table 7 Major and minor element composition of treated soils of Odisha

Compounds	1T	2T	3T	4T	5T	6T
CO_2	1.00 ± 0.01	4.93 ± 0.32	1.31 ± 0.12	1.11 ± 0.10	3.64 ± 0.38	2.38 ± 0.52
Na_2O	0.00 ± 0.00	0.77 ± 0.03	0.47 ± 0.21	0.40 ± 0.13	0.00 ± 0.00	0.00 ± 0.00
MgO	0.54 ± 0.09	0.49 ± 0.05	0.35 ± 0.13	0.00 ± 0.00	1.40 ± 0.27	1.22 ± 0.04
Al_2O_3	6.74 ± 0.44	5.88 ± 0.05	9.74 ± 0.68	11.78 ± 0.70	14.56 ± 0.96	14.02 ± 0.91
SiO_2	65.91 ± 6.78	71.12 ± 1.71	59.57 ± 6.02	67.64 ± 3.39	63.24 ± 2.83	64.55 ± 5.67
P_2O_5	0.32 ± 0.01	0.22 ± 0.09	1294.46 ± 231.57	0.59 ± 0.48	0.0 ± 0.00	0.0 ± 0.00
S	0.00 ± 0.00	188.82 ± 57.55	184.04 ± 53.81	0.00 ± 0.00	0.0 ± 0.00	0.0 ± 0.00
Cl	0.00 ± 0.00	71.74 ± 11.03	438.33 ± 48.85	368.46 ± 50.00	202.14 ± 15.53	174.27 ± 55.36
K_2O	1.13 ± 0.10	1.66 ± 0.34	3.13 ± 0.52	2.48 ± 0.17	2.45 ± 0.40	2.34 ± 0.56
CaO	1.21 ± 0.37	1.27 ± 0.48	0.64 ± 0.18	0.66 ± 0.07	0.63 ± 0.28	0.62 ± 0.21
TiO_2	3.81 ± 0.70	2.08 ± 0.12	1.11 ± 0.19	1.78 ± 0.10	1.09 ± 0.49	1.01 ± 0.19
MnO	981.82 ± 22.60	1111.48 ± 1.97	1024.09 ± 41.96	844.13 ± 77.14	0.48 ± 0.37	0.51 ± 0.33
Fe_2O_3	5.38 ± 2.39	1.69 ± 0.92	2.80 ± 0.53	2.75 ± 0.20	7.25 ± 1.33	7.37 ± 1.98
Ni	18.49 ± 1.54	15.05 ± 2.09	13.27 ± 2.26	15.55 ± 0.44	71.89 ± 2.69	63.34 ± 1.49
Cu	26.92 ± 1.55	25.86 ± 2.69	20.40 ± 2.38	21.96 ± 0.05	48.98 ± 11.01	43.52 ± 1.31
ZnO	36.56 ± 3.65	42.05 ± 2.60	46.84 ± 8.09	63.48 ± 1.15	74.64 ± 2.09	67.16 ± 4.90
B	1.04 ± 0.07	1.18 ± 0.07	12.22 ± 0.52	12.77 ± 1.00	19.83 ± 1.98	14.87 ± 2.22
Mo	39.55 ± 8.91	39.53 ± 3.22	22.52 ± 0.75	3.18 ± 0.55	2.78 ± 0.69	1.36 ± 0.34
Se	0.0 ± 0.00	0.0 ± 0.00	189.64 ± 60.77	187.36 ± 7.73	0.00 ± 0.00	0.0 ± 0.00

Mean concentration ± SD

3.1.6 EDXRF analysis

The nutritive parameters of yields is represented by the biogeochemical appearance of the dirt, the limits of vegetation has to accumulation of components and ecological contamination [20, 76]. Investigating the macro and micronutrients has imperative to plant science experts and scientists for soil profiling and crop development. In this study, mean concentration of 19 nutrients were analyzed. Among the essential macronutrients phosphorus (P), sulfur (S), nitrogen (N), calcium (Ca), potassium (K), magnesium (Mg), and some micronutrients manganese (Mn), iron (Fe), molybdenum (Mo), zinc (Zn), copper (Cu), chlorine (Cl), boron (B), cobalt (Co) were focused. In depth soil of Balasore, 15 compounds were found followed by upper soil 18 compounds, while the highest numbers (19) of compounds were found in lower soil of Ganjam followed by upper soil (17) and similar numbers of compounds were seen in lower and upper soils of Puri districts (Tables 6 and 7). CO_2, Al_2O_3, SiO_2, K_2O, CaO, TiO_2, MnO, Fe_2O_3, Ni, Cu, ZnO and B were seen in all the sites where as few concentrations of Se was found only in upper and lower sites of Ganjam soil. MnO concentration was higher in lower and upper soil of Balasore followed by SiO_2 while in Ganjam lower soil had maximum P_2O_5 followed by MnO, Cl and S. In upper soil, MnO was seen maximally followed by Cl and SiO_2. In depth soil of Puri, Cl was found in the highest concentration followed by Ni, ZnO, SiO_2 and Cu but Cl was maximum in upper soil of Puri (Table 6). After H_2O_2 treatment, MnO also maximum in upper and lower soil of Balasore and upper soil of Ganjam while P_2O_5 and MnO is the highest in Ganjam lower soil. Cl shown high concentration in lower and upper soils of Puri followed by Ni, ZnO, SiO_2 and Cu (Table 7).

3.2 Water sampling and analysis

The physicochemical properties of water samples of different coastal areas of Odisha are tabulated in Tables 8 and 9. All physical parameters of water were most essential for betel vine yard and had significant impact on growth of crop vegetation. Low and average temperature are necessary for Betel vine cultivation. So,

Table 9 Total carbon, total organic carbon, inorganic carbon, and overall nitrogen content of water used in betel vine cultivation of Odisha

Sample name	Mean concentration ± SD			
	TOC (ppm)	TC (ppm)	IC (ppm)	TN (ppm)
MQ	0.71 ± 0.27	1.53 ± 0.22	0.82 ± 0.21	0.00 ± 0.00
BAL	15.12 ± 1.04	52.27 ± 0.63	37.14 ± 0.62	0.27 ± 0.04
PUR	3.19 ± 0.78	29.28 ± 0.41	26.09 ± 0.52	0.99 ± 0.04
GAN	1.94 ± 0.44	9.54 ± 0.30	7.60 ± 0.30	0.25 ± 0.16

coastal area climate of Odisha posed as suitable place for betel growth. The temperature ranged from 18 to 22 °C in Balasore, 19 to 22 °C in Ganjam and 17 to 20 °C in Puri district (Table 8).

3.2.1 TOC-TN analysis

The mean concentration along with standard deviation (SD) of total organic carbon (TOC), total carbon (TC), inorganic carbon (IC), and total nitrogen (TN) of BAL, PUR and GAN are depicted in Table 9. Overall concentrations of TOC are higher in BAL (15.12 ± 1.04) than PUR and GAN. Similarly TC and IC of BAL waters are maximum among all other sites. Total nitrogen (TN) of PUR samples are higher followed by GAN due to open and pond water systems. Minimum concentration of TOC, TC, IC, and TN are found in GAN sites due to industrial site and poor quality of cultivation method.

4 Discussions

Soil profile alterations within agro field influence the crop production as texture majorly affect productivity and management strategies. Irrigation is closely related to soil type and water holding capacity [77]. Now days, Soil texture varies because of supplement lost [56]. However, yield capacity of sandy soils are maximum than clay soils. Soil textures also affect pest management [20, 55, 56]. Temperature fluctuation in soils is because of more warmth limit and less heat conductivity of the soil [77]. At certain period, when top soil shows more heat during day time and less heat during night, soil and air temperature

Table 8 Physiochemical properties of water use in betel vine cultivation of Odisha

Site	PH ± SD	Turbidity (NTU) ± SD	EC (μs/cm) ± SD	TDS(ppm) ± SD	Temp (°C) ± SD
BAL	6.82 ± 0.12	2 ± 1	537 ± 38.74	359.79 ± 25.96	19 ± 2
PUR	6.53 ± 0.48	6 ± 1	639.33 ± 57.33	428.35 ± 38.41	20 ± 2
GAN	7.14 ± 0.56	9 ± 1	655.67 ± 66.58	439.3 ± 44.61	26 ± 3

considerably differ for few times [49]. There is evidence of some extensive sensitive plants whose root improvement in less temperature soil [78], yet no authentication was started for root development in low temperature in comparison with hot [79]. Hence, the physicochemical parameters of soil were explored to get more information about morphological and genetical variation of betel leaves. This examination additionally gives progressively required data about ecological impacts influence on plant physiology. There are number of strategies are adopted to recognize the minerals by the conventional techniques such as X-ray diffraction, FTIR spectroscopy, and slim segment examination [6]. The FTIR studies of soils of different coastal districts of Odisha shows the various minerals present in soils as major constituents and in different compositions. The present outcomes also highlight the increased and decreased level of peak heights, which corresponds with the variation between treated and untreated samples. Coastal zones have significant soil and shoreline sands which contain the essential minerals aggregations. Mineralogical stores are the convergence of significant minerals got from the weathering of various rock gathered by wind or water [17, 69]. The FTIR range was utilized to demarcate the idea of useful gatherings which could impact the adsorption of the soil. The non destructive FTIR and XRD techniques can be utilized in the recognizable proof of mineralogical structure [11]. XRD examined on topographical entities illuminate the mineralogical changes subsequent to long term. From XRD analysis, many minerals are additionally identified which were not identified in FTIR spectroscopy. It is furthermore contemplated the crystalline characters of mineralogical composition of quartz matched with FTIR spectral pattern. So, XRD method is nondestructive and used in the identification of mineralogical composition [58, 80–82]. SEM with EDS (energy-dispersive X-ray spectroscopy) study is generally employed for uni-particle study. It provides useful information on the morphology and elemental composition of coastal soil samples [11]. The changes of microstructural variation of soils also studied by SEM microscopy [53]. The mineralogical properties and soil surface profile of coastal Odisha constitute a useful guide for proper cultivation of betel vine for its high mineralogical and nutritional value. For soil surface variation study, SEM–EDS is a precious tool. The differences of essential elemental composition constitute the multiplicity of textural nature of various coastal zones which is significant for the examination. Various micronutrients (Mn, Fe, Cu, and Zn) and macronutrients (P, K and N) are significant soil components that manage its richness [34]. In agroecosystem, catch crops are planted for better uptake of available nutrients in the soil [83]. Catch crops also enhance the biogeochemical cycling which is

a signature of characteristic soil porosity, water holding capacity, aggregate stability and growth of microbial population [84]. Many other catch crops (e.g. turnip, radish, barley, clover, groundnut, oat) can fix nitrogen and enrich organic matter in the soil [85, 86]. Corn is used as catch crop in different plant densities in a green house because of the characteristic nutrient salt uptake associated with water use [87]. Thus, *Piper betle* L. can be used as a catch crop in coastal areas for optimal utilization of nutrients. The perennial stout twining climbers of *Piper betle* strongly hold the soil of sandy loam and heavy clayey loam type soils because of the adventitious roots arising from the nodes. *Piper betle* plantations in loamy soils of coastal areas not only act as suitable environment for nutrient assimilation but also strengthen the economic productivity. Additionally, the roots of *Piper betle* L. species stabilized the soil aggregates and control the soil erosion.

5 Conclusion

Our study highlighted that coastal climates are suitable for betel vine cultivation. The results of characterization of soil help for more harvesting of crop which is significant for possible agri-business creation. Treatments of soil indicate reduction of carbon contents. In addition, SEM and EDS analysis gives new insight to surface morphology of soils and their variations. Nature of water considered as chemical, physical, and organic qualities in connection to their supplements, substance constituents and land condition [77–80]. The agro-water sometimes is contaminated due to organic wastes, industrial effluents, urban and rural runoff, human activity, etc. [17, 88–94]. Improving vineyard water supply can be essential [95]. As *Piper betle* species is very precious medicinal plant, this research suggested not to use contaminated water for betel cultivation. Our results also helpful for the improvement in soil and water management in the vineyards.

Availability of data and material The manuscript data was collected through field observation, sampling, and laboratory sample characterization and analysis.

Compliance with ethical standards

Conflict of interest The authors declare that they have no competing interests.

Consent for access to property for sampling Prior to sampling, permissions were procured from the respective vineyard owners for the collection of samples.

Consent for publication All property owners of the vineyards consented for the publication.

References

1. Rodrigo-Comino J, Senciales JM, Cerda A, Brevik EC (2018) The multidisciplinary origin of soil geography: a review. Earth-Sci Rev 177:114–123
2. Hiremath SC, Yadawe MS, Pujeri US, Hiremath DM, Pujar AS (2006) Physico-chemical analysis of ground water in municipal area of Bijapur (Karnataka). Curr World Environ 6:265–269
3. Sanaullah M, Usman M, Wakeel A, Cheema SA, Ashraf I, Farooq M (2020) Terrestrial ecosystem functioning affected by agricultural management systems: a review. Soil Tillage Res 196:104464
4. Yang X, Chen X, Yang X (2019) Effect of organic matter on phosphorus adsorption and desorption in a black soil from Northeast China. Soil Tillage Res 187:85–91
5. Else KB, Giulia B, Zhanguo B, Rachel EC, Gerlinde DD, Ron G, Luuk F, Violette G, Thom WK, Paul M, Mirjam P, Wijnand S, Jan WG, Lijbert B (2018) Soil quality—a critical review. Soil Biol Biochem 120:105–125
6. Salih C, Ali CK, Ismail C, Uner HB, Aytekin S (2004) SEM-EDS analysis and discrimination of forensic soil. Forensic Sci Int 141:33–37
7. Luo Z, Wang G, Wang E (2019) Global subsoil organic carbon turnover times dominantly controlled by soil properties rather than climate. Nat Commun 10:3688
8. Ogle SM, Alsaker C, Baldock J, Bernoux M, Breidt FJ, McConkey B, Regina K, Amabile GGV (2019) Climate and soil characteristics determine where no-till management can store carbon in soils and mitigate greenhouse gas emissions. Sci Rep 9:11665
9. He J, Shi Y, Zhao J, Yu Z (2019) Strip rotary tillage with a two year subsoiling interval enhances root growth and yield in wheat. Sci Rep 9:11678
10. Ozlu E, Sandhu SS, Kumar S, Arriaga FJ (2019) Soil health indicators impacted by long term cattle manure and inorganic fertilizer application in a corn soybean rotation of south Dakota. Sci Rep 9:11776
11. Oumabady ACN, Rajendran M, Selvaraju R (2013) FTIR spectral studies on polluted soils from industrial area at Karaikal, Puducherry state, South India. Spectrochim Acta A Mol Biomol Spectrosc 110:46–54
12. Andrews SS, Karlen DL, Mitchell JP (2002) A comparison of soil quality indexing methods for vegetable production systems in Northern California. Agr Ecosyst Environ 90:25–45
13. Nortcliff S (2002) Standardisation of soil quality attributes. Agr Ecosyst Environ 88:161–168
14. Zhang L, Zhao R, Zhongkui XIE (2014) Response of soil properties and C dynamics to land use change in the west of Loess Plateau. Soil Sci Plant Nutr 60:586–597
15. Rezapour S (2013) Response of some soil attributes to different land use types in calcareous soils with Mediterranean type climate in north- west of Iran. Environ Earth Sci 71:2199–2210
16. Joseph L, Jun BM, Flora JRV, Park CM, Yoon Y (2019) Removal of heavy metals from water sources in the developing world using low-cost materials: a review. Chemosphere 229:142–159
17. Bronick CJ, Lal R (2005) Soil structure and management: a review. Geoderma 124:3–22
18. Jankowski M, Przewoźna B, Bednarek R (2011) Topographical inversion of sandy soils due to local conditions in Northern Poland. Geomorphology 135:277–283
19. Quesada HB, Baptista ATA, Cusioli LF, Seibert D, Bezerra O, Bergamasco R (2019) Surface water pollution by pharmaceuticals and an alternative of removal by low cost adsorbents: a review. Chemosphere 222:766–780
20. Usowicz B, Lipiec J (2017) Spatial variability of soil properties and cereal yield in a cultivated field on sandy soil. Soil Tillage Res 174:241–250
21. Yu Q, Hu X, Ma J, Ye J, Sun W, Wang Q, Lin H (2020) Effect of long-term organic material applications on soil carbon and nitrogen fractions in paddy fields. Soil Tillage Res 196:104483
22. Pedrera-Parrilla A, Brevik EC, Giráldez JV, Vanderlinden K (2016) Temporal stability of electrical conductivity in a sandy soil. Int Agrophys 30:349–357
23. Ozpinar S, Cay A (2006) Effect of different tillage systems on the quality and crop productivity of a clay-loam soil in semi-arid north-western Turkey. Soil Tillage Res 88:95–106
24. Ozpinar S, Ozpinar A (2015) Tillage effects on soil properties and maize productivity in western Turkey. Arch Agron Soil Sci 61:1029–1040
25. Gałka B, Kabała C, Karczewska A, Sowiński J (2016) Variability of soil properties in an intensively cultivated experimental field. Soil Sci Annu 67:10–16
26. Awe GO, Reichert JM, Timm LC, Wendroth OO (2015) Temporal processes of soil water status in a sugarcane field under residue management. Plant Soil 387:395–411
27. Gajda A, Czyż E, Dexter A (2016) Effects of long-term use of different farming systems on some physical, chemical and microbiological parameters of soil quality. Int Agrophys 30:165–172
28. Aranyos J, Tomócsik A, Makádi M, Mészáros J, Blaskó L (2016) Changes in physical properties of sandy soil after long-term compost treatment. Int Agrophys 30:269–274
29. Bruno MS, Geraldo CO, Milson ES, Érika AS, Paulo TGG, Laura BBM, Lloyd DN, Nilton C (2019) Soil moisture associated with least limiting water range, leaf water potential, initial growth and yield of coffee as affected by soil management system. Soil Tillage Res 189:36–43
30. Ikabongo M, Mariko S, Ryusuke H (2019) Short-term land-use change from grassland to cornfield increases soil organic carbon and reduces total soil respiration. Soil Tillage Res 186:1–10
31. Haddaway NR, Hedlund K, Jackson LE, Katterer T, Lugato E, Thomsen IK, Helene BJ, Isberg P (2017) How does tillage intensity affect soil organic carbon? A systematic review. Environ Evid 6:30
32. Di Vita G, Pilato M, Pecorino B, Brun F, D' Amico M (2017) A review of the role of vegetal ecosystems in CO_2 capture. Sustainability 9:1840
33. Paul BLG, Delphine L, Simon C, Fiona MS, John GK, Richard ME, Robert IG, Inma L, Bridget AE, David AR, Davey LJ (2019) Divergent national-scale trends of microbial and animal biodiversity revealed across diverse temperate soil ecosystems. Nat Commun 10:1107

34. Sugihara S, Shibata M, Ze AD, Tanaka H, Kosaki T, Funakawa S (2019) Forest understories controlled the soil organic carbon stock during the fallow period in African tropical forest: a ^{13}C analysis. Sci Rep 9:9835

35. Sian Kou G, Duncan M (2019) Nitrogen-fixing trees could exacerbate climate change under elevated nitrogen deposition. Nat Commun 10:1493

36. Jorg S, Samuel F, Hanna J, Martin O, Mathias G, Britta PF, Stefan P, Benjamin G, Bo E (2019) Silicon increases the phosphorus availability of Arctic soils. Sci Rep 9:449

37. Jaafar HH, Ahmad FA, Beyrouthy NE (2019) GCN250, new global gridded curve numbers for hydrologic modeling and design. Sci Data 6:145

38. Cernusak LA, Ubierna N, Winter K, Holtum JA, Marshall JD, Farquhar GD (2013) Environmental and physiological determinants of carbon isotope discrimination in terrestrial plants. New Phytol 200:950–965

39. Dubber D, Gray NF (2010) Replacement of chemical oxygen demand (COD) with total organic carbon (TOC) for monitoring wastewater treatment performance to minimize disposal of toxic analytical waste. J Environ Sci Health 45:1595–1600

40. Fadini PS, Jardim WF, Guimaraes JR (2004) Evaluation of organic load measurement techniques in sewage and waste stabilization pond. J Braz Chem Soc 15:131–135

41. Knapik HG, Fernandes CVS, Azevedo JCR, Porto MFA (2014) Applicability of fluorescence and absorbance spectroscopy to estimate organic pollution in rivers. Environ Eng Sci 31:653–663

42. Yu Z, Wang X, Han G, Liu X, Zhang E (2018) Organic and inorganic carbon and their stable isotopes in surface sediments of the yellow river estuary. Sci Rep 8:10825

43. Chen S, Li S, Ma W, Ji W, Xu D, Shi Z, Zhang G (2018) Rapid determination of soil classes in soil profiles using vis-NIR spectroscopy and multiple objectives mixed support vector classification. Eur J Soil Sci 70:42–53

44. Huyssteen CW, Turner DP, Roux P (2013) Principles of soil classification and the future of the South African system. S Afr J Plant Soil 30:23–32

45. Olson KR, Al-Kaisi MM (2015) The importance of soil sampling depth for accurate account of soil organic carbon sequestration, storage, retention and loss. CATENA 125:33–37

46. Saha D, Kukal SS, Sharma S (2011) Landuse impacts on SOC fractions and aggregate stability in typic ustochrepts of Northwest India. Plant Soil 339:457–470

47. Fang X-M, Chen F-S, Wan S-Z, Yang Q-P, Shi J-M (2015) Topsoil and deep soil organic carbon concentration and stability vary with aggregate size and vegetation type in subtropical china. PLoS ONE 10(9):e0139380

48. Beretta AN, Silbermann AV, Paladino L, Torres D, Bassahun D, Musselli R, García-Lamohte A (2014) Soil texture analyses using a hydrometer: modification of the Bouyoucos method. Ciencia Investigacion Agraria 41:263–271

49. Bastida F, Garcia C, Fierer N, Eldridge DJ, Bowker MA, Abades S, Alfaro FD, Berhe AA, Cutler NA, Gallardo A, Velazquez LG, Hart SC, Hayes PE, Hernandez T, Hseu ZY, Jehmlich N, Kirchmair M, Lambers H, Neuhauser S, Victor MPR, Perez CA, Reed SC, Santos F, Siebe C, Sullivan BW, Trivedi P, Vera A, Williams MA, Moreno JL, Baquerizo MD (2019) Global ecological predictors of soil priming effect. Nat Commun 10:3481

50. Bruckman VJ, Wriessnig K (2013) Improved soil carbonate determination by FT-IR and X-ray analysis. Environ Chem Lett 11:65–70

51. Wang Q, Wang W, He X, Zheng Q, Wang H, Wu Y, Zhong Z (2017) Changes in soil properties, X-ray-mineral diffractions and infrared functional groups in bulk soil and fractions following afforestation of farmland, Northeast China. Sci Rep 7:12829

52. Pattnayak S, Kumar M, Sahu SC, Dhal NK, Behera RK (2018) Composition of soil characteristics and carbon content of contrastingly different moist-mixed deciduous and evergreen mangrove forest in Odisha, India. Geol Ecol Landsc 3(4):239–246

53. Zhou X, Liu D, Bu H, Deng L, Liu H, Yuan P, Du P, Song H (2018) XRD-based quantitative analysis of clay minerals using reference intensity ratios, mineral intensity factors, Rietveld, and full pattern summation methods: a critical review. Solid Earth Sci 3:16–29

54. Isabella B, Ines H, Michael R (2004) Determination of total organic carbon—an overview of current methods. Trends Anal Chem 23:716–726

55. Goebes P, Schmidt K, Schmidt K, Seitz S, Both S, Bruelheide H, Erfmeier A, Scholten T, Kuhn P (2019) The strength of soil plant interactions under forest is related to critical soil depth. Sci Rep 9:8635

56. Liu G, Yang J, Yao R (2006) Electrical conductivity in soil extracts: chemical factors and their intensity. Pedosphere 16:100–107

57. Rhoades JD, Corwin DL (1990) Soil electrical conductivity: effect of soil properties and application to soil salinity appraisal. Commun Soil Sci Plant Anal 21:837–860

58. Cannane NOA, Rajendran M, Selvaraju R (2013) FTIR spectral studies on polluted soils from industrial area at Karaikal, Puducherry state, South India. Spectrochim Acta Part A Mol Biomol Spectrosc 110:46–54

59. Chester R, Green RN (1968) The infrared determination of quartz in sediments and sedimentary rocks. Chem Geol 3:199–212

60. Chester R, Elderfield H (1967) The application of infrared absorption spectroscopy to carbonate mineralogy. Sedimentology 9:5–21

61. Li M, Fang C, Kawasaki S, Achal V (2018) Fly ash incorporated with biocement to improve strength of expansive soil. Sci Rep 8:2565

62. Saikia BJ, Parthasarthy G (2010) Fourier transform infrared spectroscopic characterization of Kaolinite from Assam and Meghalaya, Northeastern India. J Mod Phy 1:206–210

63. Ramasamy V, Rajkumar P, Ponnusamy V (2009) Depth wise analysis of recently excavated Vellar river sediments through FTIR and XRD studies. Indian J Phys 83:1295–1380

64. Cannane NOA, Rajendran M, Selvaraju R (2014) Minerological identification of polluted soils using XRD method. J Environ Nanotechnol 3:23–29

65. Collins K (1983) Scanning electron microscopy of engineering soils. Geoderma 30:243–252

66. Gvirtzman H, Magaritz M, Klein E, Nadler A (1987) A Scanning Electron Microscopy study of water in soil. Transp Porous Media 2:83–93

67. Sergeyev EM, Spivak GV, Osipov VI, Rau EI, Sokolov VN, Filippov MN (1980) The application of the SEM in the study of soils. Scanning 3:262–272

68. Ivanov K, Penka Z, Violina A, Stefan K (2019) Scanning Electron Microscopy and X-ray Diffraction in the determination of macroelements in soil and plants. Commun Soil Sci Plant Anal 50:878–893

69. Sajitha SS, Nisha RB, Metilda P, Jenin GA (2018) FTIR, XRD, SEM/EDAX analysis of coastal soil samples of Kanyakumari district in full moon and new moon day. Int J Adv Res 6:1109–1115

70. Chang I, Cho G (2019) Shear strength behavior and parameters of microbial gellan gum-treated soils: from sand to clay. Acta Geotech 14:361–375

71. Veghte D, Freedman A (2014) Facile method for determining the aspect ratios of mineral dust aerosol by electron microscopy. Aerosol Sci Technol 48:715–724

72. Jeong GY, Nousiainen T (2014) Tem analysis of the internal structures and mineralogy of asian dust particles and the implications for optical modeling. Atmos Chem Phys 14:7233–7254

73. Stefanie NF, Matthew DL, Kyle JR, Zhao D (2015) Scanning electron microscopy cathodoluminescence of quartz: principles, techniques and applications in ore geology. Ore Geol Rev 65:840–852

74. Gobac ZZ, Posilovic H, Bermanee V (2009) Identification of biogenetic calcite and aragonite using SEM. Geol Croat 62:201–206

75. Liu Y, Li Y, Li Q, Bao J, Hao D, Zhao Z, Song D (2015) Micro- to nanoscale morphologies and chemical components of soils investigated by SEM-EDS for forensic science. J Chem. https://doi.org/10.1155/2015/734560

76. Tezotto T, Favarin JL, Neto AP, Gratao PL, Azevedo RA, Mazzafera P (2013) Simple procedure for nutrient analysis of coffee plant with energy dispersive X-ray fluorescence spectrometry (EDXRF). Scientia Agricola 70:263–267

77. Zhu D, Ciais P, Krinner G, Maignan F, Puig AJ, Hugelius G (2019) Control of soil organic matter on soil thermal dynamics in the northern high latitudes. Nat Commun 10:3172

78. Schenker G, Lenz A, Körner C, Hoch G (2014) Physiological minimum temperatures for root growth in seven common european broad-leaved tree species. Tree Physiol 34:302–313

79. Alvarez-Uria P, Körner C (2007) Low temperature limits of root growth in deciduous and evergreen temperate tree species. Funct Ecol 21:211–218

80. Keesstra SD, Bouma J, Wallinga J, Tittonell P, Smith P, Cerda A, Montanarella L, Quinton JN, Pachepsky Y, Van der Putten WH, Bardgett RD, Moolenaar S, Mol G, Jansen B, Fresco LO (2016) The significance of soils and soil science towards realization of the United Nations Sustainable Development Goals. Soil 2:111–128

81. Keesstra S, Mol G, de Leeuw J, Okx J, Molenaar C, de Cleen M, Visser S (2018) Soil-related sustainable development goals: four concepts to make land degradation neutrality and restoration work. Land 7:133

82. Novara A, Pulido M, Rodrigo-Comino J, Di Prima S, Smith P, Gristina L, Giminez-morera A, Terol E, Salesa D, Keesstra S (2019) Long-term organic farming on a citrus plantation results in soil organic matter recovery. Cuadernos de Investigación Geográfica. 45:271–286

83. Ding G, Liu X, Herbert S, Novak J, Amarasiriwardena D, Xing B (2006) Effect of cover crop management on soil organic matter. Geoderma 130:229–239

84. Gabriel JL, Muñoz-Carpena R, Quemada M (2012) The role of cover crops in irrigated systems: water balance, nitrate leaching and soil mineral nitrogen accumulation. Agric Ecosyst Environ 155:50–61

85. Storr T, Simmons RW, Hannam JA (2019) A UK survey of the use and management of cover crops. Ann Appl Biol 174:179–189

86. Abdalla M, Hastings A, Cheng K, Yue Q, Chadwick D, Espenberg M, Truu J, Rees RM, Smith P (2019) A critical review of the impacts of cover crops on nitrogen leaching, net greenhouse gas balance and crop productivity. Glob Change Biol 25:2530–2543

87. Yasutake D, Kiyokawa C, Kondo K, Nomiyama R, Kitano M, Mori M, Yamane S, Maeda M, Nagare H, Fujiwara T (2014) Characteristics of nutrient salt uptake associated with water use of corn as a catch crop at different plant densities in a greenhouse. Pedosphere 24:339–348

88. Behera SK, Shukla AK (2015) Spatial distribution of surface soil acidity, electrical conductivity, soil organic carbon content and exchangeable potassium calcium and magnesium in some cropped acid soils of India. Land Degrad Dev 26:71–79

89. Behera SK, Singh MV, Singh KN, Todwal S (2011) Distribution variability of total and extractable zinc in cultivated acid soils of India and their relationship with some selected soil properties. Geoderma 162:242–250

90. Basso B, Cammarano D, Fiorentino C, Ritchie JT (2013) Wheat yield response to spatially variable nitrogen fertilizer in Mediterranean environment. Eur J Agron 51:65–70

91. Di Prima S, Rodrigo-Comino J, Novara A, Iovino M, Pirastru M, Keesstra S, Cerdà A (2018) Soil physical quality of citrus orchards under tillage, herbicide, and organic managements. Pedosphere 28:463–477

92. Cerdà A, Ackermann O, Terol E, Rodrigo-Comino J (2019) Impact of farmland abandonment on water resources and soil conservation in citrus plantations in eastern Spain. Water 11:824

93. Surarak C, Likitlersuang S, Wanatowski D, Balasubramaniam A, Oh E, Guan H (2012) Stiffness and strength parameters for hardening soil model of soft and stiff Bangkok clays. Soils Found 52:682–697

94. Liu XA, Finley BK, Mau RL, Schwartz E, Dijkstra P, Bowker MA, Hungate BA (2020) The soil priming effect: consistent across ecosystem, elusive mechanisms. Soil Biol Biochem 140:107617

95. Medrano H, Tomas M, Martorell S, Escalona J, Pou A, Fuentes S, Flexas J, Bota J (2015) Improving water use efficiency of vineyards in semi-arid regions. A review. Agron Sustain Dev 35:499–517